Atmos. Chem. Phys. Discuss., 7, 2169–2196, 2007
www.atmos-chem-phys-discuss.net/7/2169/2007/

Atmospheric
Chemistry
and Physics
Discussions

A semi-analytical method for calculating rates of new sulfate aerosol formation from the gas phase

J. Kazil[1,2] **and E. R. Lovejoy**[1]

[1]NOAA Earth System Research Laboratory, Boulder, CO, USA
[2]National Research Council Associateship Program, Washington, D.C., USA

Received: 8 January 2007 – Accepted: 30 January 2007 – Published: 15 February 2007

Correspondence to: J. Kazil (jan.kazil@noaa.gov)

Abstract

The formation of new sulfate aerosol from the gas phase is commonly represented in atmospheric modeling with parameterizations of the steady state nucleation rate. Such parameterizations are based on classical nucleation theory or on aerosol nucleation rate tables, calculated with a numerical aerosol model. These parameterizations reproduce aerosol nucleation rates calculated with a numerical aerosol model only imprecisely. Additional errors can arise when the nucleation rate is used as a surrogate for the production rate of particles of a given size. We discuss these errors and present a method which allows a more precise calculation of steady state sulfate aerosol formation rates. The method is based on the semi-analytical solution of an aerosol system in steady state and on parameterized rate coefficients for H_2SO_4 uptake and loss by sulfate aerosol particles, calculated from laboratory and theoretical thermodynamic data.

1 Introduction

Sulfate aerosol particles play an important role in Earth's atmosphere: They scatter solar radiation, facilitate heterogeneous and aqueous chemistry, and act as condensation and ice nuclei for the formation of clouds, one of the most important elements in the climate system. A dependable representation of sulfate aerosol in atmospheric modeling is therefore essential for the understanding of the Earth's atmosphere. The formation of new sulfate aerosol from the gas phase is commonly represented by parameterizations of the steady state nucleation rate. Aerosol nucleation is the process by which supercritical molecular clusters, particles larger than the critical cluster, form from gas phase molecules. The critical cluster is the smallest particle whose growth due to uptake of gas phase molecules is uninhibited by a thermodynamic barrier. Steady state parameterizations of the sulfate aerosol nucleation rate rest upon the determination of the surface tension of small clusters of given H_2SO_4 and H_2O contents (e.g. Vehkamäki et al., 2002), or on tabulated nucleation rates, calculated with a numerical aerosol

Title Page
Abstract | Introduction
Conclusions | References
Tables | Figures
◀| |▶
◀ ▶
Back | Close
Full Screen / Esc
Printer-friendly Version
Interactive Discussion
EGU

model (e.g. Modgil et al., 2005). These parameterizations reproduce aerosol formation rates calculated with numerical aerosol models with a limited precision. Independently of the precision of these parameterizations, errors can arise when the nucleation rate is used as a surrogate for the production rate of particles of a given size. We discuss these errors and present a method which allows a more precise calculation of steady state sulfate aerosol formation rates. The method employs a semi-analytical solution of an aerosol system in steady state, parameterized rate coefficients for H_2SO_4 and H_2O uptake and loss by the aerosol particles, and calculated rate coefficients for the coagulation of the aerosol particles among themselves and with preexisting aerosol. Advantages of our approach are the representation of the physical processes leading to new aerosol formation, the use of laboratory thermodynamic data for the initial steps of cluster formation, absence of numerical diffusion, and a high precision, reflected in small deviations from particle formation rates calculated with a numerical aerosol model.

2 Neutral and charged sulfate aerosol formation

The scheme of neutral and charged H_2SO_4/H_2O aerosol formation from the gas phase is shown in Fig. 1: The ionization rate q is the rate at which the anions A_0^- and the cations A^+ are produced. Here we assume that $A_0^- = NO_3^-(HNO_3)$. The neutral and charged clusters A_i and A_i^- are defined as

$$\begin{aligned} A_i &= (H_2SO_4)_i(H_2O)_{\overline{x}(i)} \\ A_i^- &= HSO_4^-(H_2SO_4)_{i-1}(H_2O)_{\overline{y}(i)} \end{aligned} \quad , \quad i = 1, \ldots, n \quad . \tag{1}$$

$\overline{x}(i)$ and $\overline{y}(i)$ are the average H_2O contents of the clusters in equilibrium with respect to H_2O uptake and loss. A_1 is, as a matter of course, gas phase sulfuric acid, which we will denote in the following simply with H_2SO_4. The clusters grow and evaporate with

Title Page
Abstract | Introduction
Conclusions | References
Tables | Figures
◀◀ | ▶▶
◀ | ▶
Back | Close
Full Screen / Esc
Printer-friendly Version
Interactive Discussion

the first order rate coefficients

$$\kappa_i = k_{a_i} \cdot [H_2SO_4] \quad , \quad \lambda_i = k_{d_i} \quad ,$$
$$\kappa_i^- = k_{a_i}^- \cdot [H_2SO_4] \quad , \quad \lambda_i^- = k_{d_i}^- \quad . \tag{2}$$

k_{a_i} and k_{d_i} are the H_2SO_4 uptake and evaporation rate coefficients of the A_i, $k_{a_i}^-$ and $k_{d_i}^-$ the H_2SO_4 uptake and evaporation rate coefficients of the A_i^-, averaged over the equilibrium H_2O distribution of the clusters. The ω_i and ω_i^- in Fig. 1 are the pseudo first order rate coefficients for loss of the A_i and A_i^- by coagulation among each other and onto preexisting aerosol. The p_i and p_i^- are production rates of the A_i and A_i^- by coagulation of smaller clusters. The α_i are pseudo first order rate coefficients for the recombination of the A_i^- with the cations A^+. The rate coefficients and their calculation are explained in more detail in Sect. 3.

We denote the net steady state formation rate of the A_i and A_i^- with $i > n$ from the A_i and A_i^- with $i \leq n$ with $\mathcal{J}(n, p, q, r, s, t, [H_2SO_4])$. $\mathcal{J}$ is a function of pressure p, ionization rate q, relative humidity r, H_2SO_4 condensational sink s, temperature t, and of the sulfuric acid gas phase concentration $[H_2SO_4]$. The pressure dependence of $\mathcal{J}$ is weak if the clusters A_i and A_i^- with $i \leq n$ are much smaller than the mean free path of gas phase molecules (typically > 100 nm in atmospheric conditions), when their H_2SO_4 uptake and loss as well as their coagulation take place in the free molecular regime. $\mathcal{J}$ can be broken down into three contributions,

$$\mathcal{J}(n, p, q, r, s, t, [H_2SO_4]) = J_{cond} + J_{evap} + J_{coag} \quad , \tag{3}$$

where

$$J_{cond} = k_{a_n}[H_2SO_4][A_n] + k_{a_n}^-[H_2SO_4][A_n^-] \tag{4}$$

represents for the formation of clusters by condensation of sulfuric acid,

$$J_{evap} = -k_{d_{n+1}}[A_{n+1}] - k_{d_{n+1}}^-[A_{n+1}^-] \tag{5}$$

the loss of clusters by evaporation of sulfuric acid, and

$$
\begin{aligned}
J_{\mathrm{coag}} = & \sum_{i=2}^{n} \sum_{j=\max(i,n+1-i)}^{n} k_{c_{i,j}}[\mathrm{A}_i][\mathrm{A}_j] \\
& + \sum_{i=2}^{n} \sum_{j=n+1-i}^{n} k^{-}_{c_{i,j}}[\mathrm{A}_i][\mathrm{A}^{-}_j]
\end{aligned}
\tag{6}
$$

the formation of clusters due to coagulation. The calculation of the coagulation rate coefficients $k_{c_{i,j}}$ and $k^{-}_{c_{i,j}}$ is explained in Sect. 3.

The smallest neutral cluster whose sulfuric acid content c satisfies

$$
\begin{aligned}
& k_{a_c} \cdot [\mathrm{H_2SO_4}] \geq k_{d_c} \\
\wedge \quad & k_{a_i} \cdot [\mathrm{H_2SO_4}] > k_{d_i} \quad \forall\, i > c
\end{aligned}
\tag{7}
$$

is the neutral critical cluster. For $n \gg c$, the particles A_{n+1} and A^{-}_{n+1} evaporate only very slowly, and $J_{\mathrm{evap}} \approx 0$. Atmospheric models which account for H_2SO_4/H_2O particles containing more than n H_2SO_4 molecules need to be supplied only with the formation rate

$$
J(n,p,q,r,s,t,[\mathrm{H_2SO_4}]) = J_{\mathrm{cond}} + J_{\mathrm{coag}} \tag{8}
$$

of these particles, since they can either neglect J_{evap} if $n \gg c$, or otherwise calculate it from the concentrations of the particles they account for. We therefore focus in the following on the particle formation rate $J(n,p,q,r,s,t,[\mathrm{H_2SO_4}])$, which we will refer to as nucleation rate for $n=c$.

3 Rate coefficients

The rate coefficients for sulfuric acid uptake by the neutral and charged H_2SO_4/H_2O aerosol particles are calculated with the Fuchs formula for Brownian coagulation

(Fuchs, 1964; Jacobson, 1999). The effect of particle charge is accounted for as described by Lovejoy et al. (2004). The rate coefficients for sulfuric acid evaporation from the aerosol particles are calculated from the uptake rate coefficients and from the thermodynamic data for H_2SO_4 uptake/loss by the particles, described in Sect. 4. The resulting H_2SO_4 uptake and loss rate coefficients are averaged over the equilibrium probability distributions of the particle H_2O content, giving the rate coefficients k_{a_i}, k_{d_i}, $k^-_{a_i}$, and $k^-_{d_i}$. The equilibrium probability distributions of the particle H_2O content and the corresponding averages are calculated from the thermodynamic data for H_2O uptake/loss by the particles, described in Sect. 4.

The rate coefficients $k_{c_{i,j}}$ for coagulation of the neutral particles among themselves, the rate coefficients $k^-_{c_{i,j}}$ for the coagulation of neutral and charged particles, and the rate coefficients $k_{\mathrm{pre,i}}$ and $k^-_{\mathrm{pre,i}}$ for their coagulation with preexisting aerosol are calculated with the Fuchs formula. The masses and diameters of the particles used in the calculation are determined from their H_2SO_4 and average H_2O contents. The effect of the particle charge is accounted for as described by Lovejoy et al. (2004). Charging of the preexisting aerosol particles is neglected.

The pseudo first order rate coefficients ω_i and ω^-_i (Fig. 1) for loss of the particles by coagulation with each other and with preexisting aerosol are calculated with

$$\begin{aligned}\omega_i = &\sum_{j=2}^{n}(1+\delta_{i,j})k_{c_{i,j}}[\mathrm{A}_j]\\ &+\sum_{j=0}^{n}k^-_{c_{i,j}}[\mathrm{A}^-_j]+\frac{k_{\mathrm{pre,i}}}{k_{\mathrm{pre,1}}}s \quad , \quad i=1,\ldots,n \quad ,\end{aligned} \tag{9}$$

and

$$\omega^-_i = \sum_{j=2}^{n}k^-_{c_{j,i}}[\mathrm{A}_j]+\frac{k^-_{\mathrm{pre,i}}}{k_{\mathrm{pre,1}}}s \quad , \quad i=0,\ldots,n \quad , \tag{10}$$

with the preexisting aerosol H_2SO_4 condensational sink s. The summation over the neutral cluster concentrations $[A_j]$ starts with $j=2$, because coagulation with A_1 is equivalent to uptake of gas phase H_2SO_4, which is accounted for by the H_2SO_4 uptake rate coefficients. The production rates p_i of neutral clusters due to coagulation read

$$\begin{aligned} p_i &= 0 \quad , \quad i = 1, \ldots, 3 \quad , \\ p_i &= \sum_{j=2}^{i-2} \frac{1+\delta_{j,i-j}}{2} k_{c_{j,i-j}} [A_j][A_{i-j}] \quad , \\ & \quad i = 4, \ldots, n \quad . \end{aligned} \tag{11}$$

p_1 equals zero because A_1 is gas phase H_2SO_4. The $p_{i=2,3}$ equal zero, and the summation giving the $p_{i=4,\ldots,n}$ starts with 2 and ends with $i-2$ because coagulation with A_1 is equivalent to uptake of gas phase H_2SO_4, which is accounted for by the H_2SO_4 uptake rate coefficients.

The production rates p^-_i of charged clusters due to coagulation read

$$\begin{aligned} p^-_1 &= 0 \quad , \\ p^-_i &= \sum_{j=0}^{i-2} k^-_{c_{i-j,j}} [A_{i-j}][A^-_j] \quad , \quad i = 2, \ldots, n \quad . \end{aligned} \tag{12}$$

p^-_1 equals zero and the summation giving the $p^-_{i=2,\ldots,n}$ ends with $i-2$ because coagulation with A_1 is equivalent to uptake of gas phase H_2SO_4, which is accounted for by the H_2SO_4 uptake rate coefficients.

The pseudo first order rate coefficients $\alpha_i = k_{r_i}[A^+]$ describe the recombination of the A^-_i with cations A^+, where the k_{r_i} are the rate coefficients for recombination of the anions with the cation population. A mass and size independent recombination rate coefficient $k_{r_i} \doteq k_r = 1.6 \cdot 10^{-6}$ cm^3 s^{-1} (Bates, 1982) is assumed for all anions/cations in this work.

In atmospheric conditions, the mean free path of gas phase molecules is typically >100 nm. H_2SO_4 uptake and loss as well as the coagulation of particles much smaller than this size take place in the free molecular regime, where the corresponding rate coefficients are essentially independent of pressure. All rate coefficients were therefore calculated at 1013.25 hPa. The water vapor saturation pressure formulation by Goff (1957) was used in all calculations to transform relative humidity over water to water vapor concentration and vice versa.

4 Thermodynamic data for H_2SO_4 and H_2O uptake and loss

The thermodynamic data for uptake and loss of H_2SO_4 and H_2O by the small charged clusters are based on the laboratory measurements of Curtius et al. (2001) and of Froyd and Lovejoy (2003). The thermodynamic data for the formation of $(H_2SO_4)_2(H_2O)_{\bar{x}(2)}$ and of $(H_2SO_4)_3(H_2O)_{\bar{x}(3)}$ are calculated explicitly from fits to the laboratory measurements by Hanson and Lovejoy (2006). These fits read, with RH over water in %,

$$\begin{aligned} dS(\mathrm{kcal\ mol^{-1}\ K^{-1}}) &= -0.04 \\ dH(\mathrm{kcal\ mol^{-1}}) &= -18.32 - 4.55\cdot 10^{-3}\cdot \mathrm{RH} \end{aligned} \tag{13}$$

for the dimer formation and

$$\begin{aligned} dS(\mathrm{kcal\ mol^{-1}\ K^{-1}}) &= -0.045 \\ dH(\mathrm{kcal\ mol^{-1}}) &= -21.41 - 2.63\cdot 10^{-2}\cdot \mathrm{RH} \end{aligned} \tag{14}$$

for the trimer formation.

The thermodynamic data for large aerosol particles derive from H_2SO_4 and H_2O vapor pressures over bulk solutions calculated with the Aerosol Inorganics Model (Carslaw et al., 1995), and from the liquid drop model. The thermodynamic data for intermediate size particles are a smooth interpolation of the data for the small and large particles. An exponential form of the correction to the liquid drop model Gibbs free energy for neutral clusters as introduced by Lovejoy et al. (2004) is used. In the present case, the correction has been adjusted to better match the dimer and trimer data in Eqs. 13 and 14: The term 3 $e^{-(m+n)/5}$ kcal/mol is added to the liquid drop Gibbs free energies for the addition of a sulfuric acid molecule to a $(H_2SO_4)_{m-1}(H_2O)_n$ cluster and for the addition of a water molecule to a $(H_2SO_4)_m(H_2O)_{n-1}$ cluster.

5 Parameterization

Calculating H_2SO_4 uptake and loss rate coefficients as described in Sect. 3 is numerically expensive due to the averaging of the rate coefficients over the cluster water content. Using parameterized rate coefficients and average cluster water contents can reduce the computational burden. We parameterize the rate coefficients k_{a_i}, k_{d_i}, $k^-_{a_i}$ and $k^-_{d_i}$ for H_2SO_4 uptake and loss by the neutral and charged clusters and the average cluster H_2O contents $\overline{x}(i)$ and $\overline{y}(i)$ as functions of temperature t and relative humidity r with a series of Chebyshev polynomials of the first kind $T_u(\bar{t})$ and $T_v(\bar{r})$ up to degrees u' and v', respectively:

$$k(t,r) \approx \tilde{k}_{u',v'}(t,r) = \sum_{u=0}^{u'} \sum_{v=0}^{v'} \alpha_{u,v} T_u\big(\bar{t}(t)\big) T_v\big(\bar{r}(r)\big) \tag{15}$$

with $\bar{t}$ and $\bar{r}$ defined as

$$\begin{aligned} \bar{t}(t) &= \frac{2t-(t_0+t_1)}{t_1-t_0} \quad , \\ \bar{r}(r) &= \frac{2r-(r_0+r_1)}{r_1-r_0} \quad , \end{aligned} \tag{16}$$

on the temperature and relative humidity intervals

$$\begin{aligned} t &\in [t_0, t_1]\,,\ t_0 = 190\ \mathrm{K}\,,\ t_1 = 300\ \mathrm{K}\,, \\ r &\in [r_0, r_1]\,,\ r_0 = 0.5\ \%\,,\ r_1 = 104\ \%\,. \end{aligned} \tag{17}$$

We determine the coefficients $\alpha_{u,v}$ for $u, v \le 20$ using an orthogonality property of the Chebyshev polynomials:

$$\begin{aligned} \alpha_{u,v} = {} & \frac{4}{\pi^2(1+\delta_{u,0})(1+\delta_{v,0})} \\ & \int_{-1}^{1} d\bar{t} \int_{-1}^{1} d\bar{r}\ k(\bar{t},\bar{r}) \frac{T_u(\bar{t})\,T_v(\bar{r})}{\sqrt{1-(\bar{t})^2}\sqrt{1-(\bar{r})^2}} \quad . \end{aligned} \tag{18}$$

We then measure the error of the approximation (15) with

$$E_{u',v'} = \max \left| \frac{\tilde{k}_{u',v'}(t,r) - k(t,r)}{k(t,r)} \right| \tag{19}$$

and determine the cutoff orders $u' \le 20$ and $v' \le 20$ which minimize $E_{u',v'}$.

6 Semi-analytical solution for aerosol schemes in steady state

6.1 Neutral aerosol

Here we give a semi-analytical solution for the steady state concentrations of the particles $A_{i=2,\ldots,n}$ in the aerosol scheme in Fig. 2, at a given concentration of the gas phase molecule A_1. The particles are produced by sources at the rates q_i and lost in sinks with the pseudo first order rate coefficients ρ_i. They grow by condensation of the gas phase molecules A_1 with the pseudo first order rate coefficients κ_i and decay by evaporation of those molecules with the pseudo first order rate coefficients λ_i. Let us start by assuming that the aerosol particles do not interact with each other (no coagulation). With the total pseudo first order rate coefficient for loss of the A_i

$$\sigma_i \doteq \kappa_i + \lambda_i + \rho_i \quad , \quad i = 2, \ldots, n \tag{20}$$

the system of differential equations for the concentrations $[A_i]$ reads

$$\begin{aligned} \frac{d[A_i]}{dt} &= q_i - \sigma_i[A_i] + \kappa_{i-1}[A_{i-1}] \\ &+ \lambda_{i+1}[A_{i+1}] \quad , \quad i = 2, \ldots, n-1 \quad , \\ \frac{d[A_n]}{dt} &= q_n - \sigma_n[A_n] + \kappa_{n-1}[A_{n-1}] \quad . \end{aligned} \tag{21}$$

The $[A_i]$ in steady state ($d[A_i]/dt = 0$) can be calculated from this system of equations with

$$[A_i] = R_{i-1}[A_{i-1}] + S_{i-1} \quad , \quad i = 2, \ldots, n \quad . \tag{22}$$

The coefficients R_i and S_i read

$$\begin{aligned} R_{n-1} &= \frac{\kappa_{n-1}}{\sigma_n} \quad , \\ R_i &= \frac{\kappa_i}{\sigma_{i+1} - \lambda_{i+2}R_{i+1}} \quad , \quad i = n-2, \ldots, 1 \quad , \\ S_{n-1} &= \frac{q_n}{\sigma_n} \quad , \\ S_i &= \frac{q_{i+1} + \lambda_{i+2}S_{i+1}}{\sigma_{i+1} - \lambda_{i+2}R_{i+1}} \quad , \quad i = n-2, \ldots, 1 \quad . \end{aligned} \tag{23}$$

Loss of the particles by coagulation among themselves can be accounted for by substituting the σ_i according to

$$\sigma_i \rightarrow \sigma_i + \sum_{j=2}^{n} (1 + \delta_{i,j}) k_{c_{i,j}} [\mathrm{A}_j] \quad , \quad i = 2, \ldots, n \quad . \tag{24}$$

Production of the particles due to coagulation of smaller particles can be accounted for by substituting the q_i according to

$$q_i \rightarrow q_i + \sum_{j=2}^{i-2} \frac{1 + \delta_{j,i-j}}{2} k_{c_{j,i-j}} [\mathrm{A}_j][\mathrm{A}_{i-j}] \quad , \quad i = 4, \ldots, n \quad . \tag{25}$$

$k_{c_{i,j}}$ is the rate coefficient for the coagulation of two particles A_i and A_j, which upon coagulation produce a particle A_{i+j}. The $[\mathrm{A}_i]$ in steady state can then be obtained by iterating the solution (22) and (23), starting e.g. with $[\mathrm{A}_i] = 0$ for $i = 2, \ldots, n$ and updating the cluster concentrations after each iteration. The $[\mathrm{A}_i]$ after the first iteration will be identical with the $[\mathrm{A}_i]$ without coagulation.

6.2 Charged aerosol

A semi-analytical solution for the steady state concentrations of the particles $\mathrm{A}^-_{i=0,\ldots,n}$ in the aerosol scheme in Fig. 3 is given here. The particles are produced by sources at the rates q^-_i and lost in sinks with the pseudo first order rate coefficients ρ^-_i. They grow by condensation of the gas phase molecules A_1 with the pseudo first order rate coefficients κ^-_i and decay by evaporation of those molecules with the pseudo first order rate coefficients λ^-_i. Due to their mutual electrostatic repulsion it is safe to assume that the particles do not coagulate. With the total pseudo first order rate coefficient for loss of the A^-_i

$$\sigma^-_i \doteq \kappa^-_i + \lambda^-_i + \rho^-_i \quad , \quad i = 0, \ldots, n \tag{26}$$

the system of differential equations for the concentrations $[\mathrm{A}_i^-]$ reads

$$\begin{aligned}\frac{d[\mathrm{A}_0^-]}{dt} &= q_0^- - \sigma_0^-[\mathrm{A}_0^-] + \lambda_1^-[\mathrm{A}_1^-] \quad ,\\ \frac{d[\mathrm{A}_i^-]}{dt} &= q_i^- - \sigma_i^-[\mathrm{A}_i^-] + \kappa_{i-1}^-[\mathrm{A}_{i-1}^-]\\ &\quad + \lambda_{i+1}^-[\mathrm{A}_{i+1}^-] \quad , \quad i = 1, \ldots, n-1 \quad ,\\ \frac{d[\mathrm{A}_n^-]}{dt} &= q_n^- - \sigma_n^-[\mathrm{A}_n^-] + \kappa_{n-1}^-[\mathrm{A}_{n-1}^-] \quad .\end{aligned} \tag{27}$$

The $[\mathrm{A}_i^-]$ in steady state $(d[\mathrm{A}_i^-]/dt = 0)$ can be calculated from this system of equations with

$$\begin{aligned}[\mathrm{A}_0^-] &= \frac{q_0^- + \lambda_1^- S_0^-}{\sigma_0^- - \lambda_1^- R_0^-} \quad ,\\ [\mathrm{A}_i^-] &= R_{i-1}^-[\mathrm{A}_{i-1}^-] + S_{i-1}^- \quad , \quad i = 1, \ldots, n \quad .\end{aligned} \tag{28}$$

The coefficients R_i^- and S_i^- read

$$\begin{aligned}R_{n-1}^- &= \frac{\kappa_{n-1}^-}{\sigma_n^-} \quad ,\\ R_i^- &= \frac{\kappa_i^-}{\sigma_{i+1}^- - \lambda_{i+2}^- R_{i+1}^-} \quad , \quad i = n-2, \ldots, 0 \quad ,\\ S_{n-1}^- &= \frac{q_n^-}{\sigma_n^-} \quad ,\\ S_i^- &= \frac{q_{i+1}^- + \lambda_{i+2}^- S_{i+1}^-}{\sigma_{i+1}^- - \lambda_{i+2}^- R_{i+1}^-} \quad , \quad i = n-2, \ldots, 0 \quad .\end{aligned} \tag{29}$$

Loss of the particles by recombination with cations can be accounted for in the system of differential Eq. (27) by substituting the σ_i^- according to

$$\sigma_i^- \rightarrow \sigma_i^- + k_{r_i} \sum_{j=0}^{n} [\mathrm{A}_j^-] \quad , \quad i = 0, \ldots, n \quad , \tag{30}$$

where $\sum_{j=0}^{n} [\mathrm{A}_j^-]$ is the cation concentration in charge equilibrium, and the k_{r_i} the rate coefficients for the recombination of the A_i^- with the cation population. The $[\mathrm{A}_i^-]$ in steady state can then be obtained by iterating the solution (28) and (29), starting e.g. with $[\mathrm{A}_i^-] = 0 \; \forall \; i$ and updating the cluster concentrations after each iteration. The $[\mathrm{A}_i^-]$ after the first iteration will be identical with the $[\mathrm{A}_i^-]$ without recombination.

6.3 Coupled neutral and charged aerosol

The semi-analytical approach can be used to solve the coupled neutral/charged aerosol scheme in Fig. 1 in steady state at a fixed gas phase concentration of sulfuric acid $[\mathrm{A}_1] = [\mathrm{H_2SO_4}]$. The solutions for the neutral and charged aerosol schemes are not iterated independently, but alternatingly: The first iteration of the charged solution is applied to the bottom portion of the scheme, giving the concentrations of the charged clusters $[\mathrm{A}_i^-]$. With these the production and loss rates of the neutral clusters A_i are calculated, and the first iteration of the neutral solution applied to the top part of the scheme, giving the concentrations $[\mathrm{A}_i]$. These are then used to calculate the production and loss rates of the A_i^-, and the next iteration of the charged solution is applied to the bottom of the scheme. Iterating the procedure until a satisfactory degree of convergence is attained yields the cluster concentrations $[\mathrm{A}_i]$ and $[\mathrm{A}_i^-]$ in steady state. The neutral and charged cluster concentrations can then be used to calculate $J(n,p,q,r,s,t,[\mathrm{H_2SO_4}])$ from Eqs. (4), (6), and (8).

7 Numerical aerosol model

We use a numerical aerosol model to calculate reference particle formation rates. The model integrates the system of differential equations for the concentrations of the neutral and charged aerosol particles $A_{i=2,\ldots,n}$ and $A^-_{i=0,\ldots,n}$ in Fig. 1 for a given set of constant parameters (pressure p, ionization rate q, temperature t, relative humidity r, preexisting aerosol H_2SO_4 condensational sink s, and gas phase sulfuric acid concentration $[H_2SO_4]=[A_1]$) until the time derivative of the aerosol concentrations falls below a given threshold. The aerosol concentrations and the formation rate $J(n,p,q,r,s,t,[H_2SO_4])$ are then assumed to be good approximations of their steady state values. Alternatively, the model can be run for a given period of time, e.g. 1200 s, a common time step in large scale atmospheric modeling.

8 Error analysis

Here we compare steady state particle formation rates $J(n,p,q,r,s,t,[H_2SO_4])$ calculated with different methods. The comparisons are performed for particle formation rates exceeding 10^{-6} cm^{-3} s^{-1}, as smaller formation rates can in general be neglected in the context of atmospheric aerosol formation. The particle formation rates are calculated on a grid of parameters covering the intervals $[2,35]$ cm^{-3} s^{-1} (ionization rate q), $[25,104]$% (relative humidity r), $[0,0.01]$ s^{-1} (preexisting aerosol H_2SO_4 condensational sink s), $[190,285]$ K (temperature t), and $[10^6,2\cdot10^8]$ cm^{-3} (sulfuric acid gas phase concentration $[H_2SO_4]$), with 7 equidistant grid points on each interval. The pressure p is set to 1013.25 hPa in all calculations, as the considered particles are much smaller than the mean free path of gas phase molecules, and their processes take place in the free molecular regime, with a negligible pressure dependence. Relative humidities below 25 %, sulfuric acid concentrations below 10^6 cm^{-3}, and temperatures above 285 K are excluded from the comparison: The numerical model described of Sect. 7 is unable reach the steady state criterion for unfavorable combinations of these parameters, when the particle formation rates are extremely small ($\ll 10^{-6}$ cm^{-3} s^{-1}), possibly due to numerical errors.

8.1 Nucleation rate as a surrogate for the formation rate of particles of a given size

In large scale atmospheric models treating sulfate aerosol, particle formation rates are usually calculated with nucleation rate parameterizations (e.g. Lauer et al., 2005; Ma and von Salzen, 2006). The smallest represented particles in these models may be larger (2–10 nm) than the neutral critical cluster, which contains only a few sulfuric acid molecules in conditions favorable for nucleation. The loss of supercritical particles smaller than the smallest represented particles due to coagulation among themselves and with larger aerosol is then neglected, leading to an overestimation of particle formation rates. The resulting errors add to the intrinsic errors of aerosol nucleation parameterizations, which may exceed a factor of 2 (Vehkamäki et al., 2002; Modgil et al., 2005). Figure 4a compares nucleation rates with formation rates of particles exceeding 2.5 nm in diameter, and illustrates the errors which may arise when the aerosol nucleation rate is used in lieu of the formation rate of larger particles: The nucleation rates markedly overestimate the >2.5 nm particle formation rates, in some cases by many orders of magnitude. The numerical aerosol model described in Sect. 7 and rate coefficients calculated as described in Sect. 3 were used in the determination of the particle nucleation and formation rates. A modified approach of calculating the formation rates of particles exceeding a given diameter D is the scaling of the nucleation rates with the factor $(d/D')^3$, where d is the diameter of the smallest supercritical particle in given conditions, and D' the diameter of the smallest particle exceeding the diameter D. This is equivalent to the assumption that the particles exceeding the diameter D form solely by coagulation, which entails conservation of the total volume of the particles. In reality, growth by condensation of vapor molecules contributes significantly to the formation of larger particles, and the scaled nucleation rates will tend to underestimate the formation rates of particles exceeding a given diameter. This is illustrated in

Fig. 4b, which compares nucleation rates scaled with $(d/D')^3$ with the formation rates of particles exceeding 2.5 nm in diameter: The majority of the scaled nucleation rates underestimate the >2.5 nm particle formation rates by up to one order of magnitude, while overestimation occurs in some cases by many orders of magnitude.

8.2 Coagulation and particle formation rates

Kerminen and Kulmala (2002) have developed an analytical method to calculate the formation rate of particles of a given size from the formation rate of particles of a smaller size. The method applies when coagulation is negligible both as a sink as well as a source of particles. However, while neglecting coagulation is a reasonable approximation in the calculation of the nucleation rate, it cannot be readily neglected when calculating the formation rate of larger particles: Figure 5a compares the nucleation rate calculated without and with coagulation. 99% of the nucleation rates calculated without coagulation lie within 29% of the nucleation rates calculated with accounting for coagulation. Figure 5b on the other hand shows the errors encountered when calculating the formation rate of particles exceeding 2.5 nm in diameter: Here, 30% of the particle formation rates calculated without coagulation deviate 100% or more from the particle formation rates calculated with coagulation. The numerical aerosol model described in Sect. 7 and rate coefficients calculated as described in Sect. 3 were used in the determination of the particle nucleation and formation rates.

8.3 Semi-analytical versus numerical particle formation rate calculation

Let us now compare the particle formation rates calculated with the semi-analytical method described in Sect. 6 with particle formation rates calculated with the numerical aerosol model described in Sect. 7. Both methods employ parameterized H_2SO_4 uptake and loss rate coefficients and average particle H_2O contents (Sect. 5). The rate coefficients for coagulation of the particles among themselves and with preexisting aerosol are calculated as described in Sect. 3. Figure 6a shows the relative deviations of the semi-analytical nucleation rates with respect to the numerical nucleation rates. The deviations are tiny: The maximum error amounts to 0.4%. 99% of the semi-analytical nucleation rates lie within 0.08% of the numerical nucleation rates, 95% within 0.01%, and 90% within 0.004%. Figure 6b shows the relative deviation of the semi-analytical formation rates of particles exceeding 2.5 nm in diameter with respect to the corresponding numerical particle formation rates. These deviations are small: The maximum error amounts to 2.0%. 99% of the semi-analytical particle formation rates lie within 0.6% of the numerical particle formation rates, 95% within 0.14%, and 90% within 0.004%. The agreement of the two methods is excellent. The semi-analytical method is faster than the numerical model when run for a time period of 1200 s instead into steady state roughly by a factor of 50 in the case of the >2.5 nm particle formation rates. A further acceleration can be achieved when requirements on precision are relaxed, e.g. by reducing the number of iterations in the semi-analytical method. The time for calculating the rate coefficients has been excluded from this comparison.

8.4 Semi-analytical particle formation rates using parameterized rate coefficients versus numerical particle formation rates using calculated rate coefficients

Here we compare particle formation rates calculated with the semi-analytical method of Sect. 6, using parameterized H_2SO_4 uptake and loss rate coefficients and average particle H_2O contents (Sect. 5), with particle formation rates calculated with the aerosol model described in Sect. 7, which uses H_2SO_4 uptake and loss rate coefficients and and average particle H_2O contents calculated from scratch (Sect. 3). The rate coefficients for coagulation of the particles among themselves and with preexisting aerosol are calculated as described in Sect. 3 by both methods. Figure 7a shows the relative deviation of the semi-analytical nucleation rates with respect to the numerical nucleation rates. The maximum error amounts to 160%. Such large deviations occur when errors in the parameterized rate coefficients lead to an erroneous determination of critical cluster H_2SO_4 content. However, only 0.7% of the errors exceed 10%, and the majority of the errors is considerably smaller: 99% of the semi-analytical nucleation rates lie within 8.0% of the numerical nucleation rates, 95% within 2.8%, and 90% within 1.3%. Figure 7b shows the relative deviation of the semi-analytical formation rates of particles exceeding 2.5 nm in diameter with respect to the corresponding numerical particle formation rates. Here the maximum error amounts to 25%, and 99% of the semi-analytical particle formation rates lie within 7.1% of the numerical particle formation rates, 95% within 2.7%, and 90% within 1.5%. The agreement of the two methods is very good. The errors seen in the semi-analytical particle formation rates are mainly due to errors in the parameterization of the H_2SO_4 uptake and loss rate coefficients. The semi-analytical method using these parameterized rate coefficients is faster than the numerical model using the rate coefficients calculated from scratch when run for a time period of 1200 s by a factor of several hundred in the case of the >2.5 nm particle formation rates. A further acceleration can be achieved when requirements on precision are relaxed, e.g. by reducing the number of iterations in the semi-analytical method, or the maximum order of the Chebyshev polynomial expansion used in the rate coefficient parameterization.

9 Conclusions

We have discussed the errors which can arise when the steady state nucleation rate is used as a surrogate for the steady state formation rate of larger aerosol particles. These errors can be substantial, exceeding an order of magnitude in some cases, and add to the errors of nucleation rate parameterizations. It is therefore recommended to assess the impact of these errors when the aerosol nucleation rate is used in lieu of the formation rate of particles of a given size. We have also presented a semi-analytical method to calculate steady state formation rates of sulfate aerosol which uses parameterized rate coefficients for sulfuric acid uptake and loss by the aerosol particles. The method reproduces aerosol formation rates calculated with a numerical aerosol model better than other methods currently used in atmospheric modeling. The method is faster than the numerical integration of the differential equations describing an aerosol scheme over a time step typically used in current medium and large scale atmospheric models. This comparison of computational expense gives only a rough measure of the efficiency of the two compared methods, however, which both can be optimized in a given setting.

Acknowledgements. This work is supported by the National Research Council and by the NOAA Climate and Global Change Program.

References

Bates, D. R.: Recombination of small ions in the troposphere and lower stratosphere, Planet. Space Sci., 30, 1275–1282, 1982. 2175

Carslaw, K. S., Clegg, S. L., and Brimblecombe, P.: A thermodynamic model of the system HCl-HNO_3-H2SO_4-H_2O, including solubilities of HBr, from <200 K to 328 K, J. Phys. Chem., 99, 11 557–11 574, 1995. 2176

Curtius, J., Froyd, K. D., and Lovejoy, E. R.: Cluster ion thermal decomposition (I): Experimental kinetics study and ab initio calculations for $HSO_4^-(H_2SO_4)_{(x)}(HNO_3)_{(y)}$, J. Phys. Chem. A, 105, 10 867–10 873, 2001. 2176

Froyd, K. D. and Lovejoy, E. R.: Experimental Thermodynamics of Cluster Ions Composed of H_2SO_4 and H_2O. 2. Measurements and ab Initio Structures of Negative Ions, J. Phys. Chem. A, 107, 9812–9824, 2003. 2176

Fuchs, N. A.: The Mechanics of Aerosols, Macmillan, 1964. 2174

Goff, J. A.: Saturation pressure of water on the new Kelvin temperature scale, in: Transactions of the American Society of Heating and Ventilating Engineers, pp. 347–354, American Society of Heating and Ventilating Engineers, 1957. 2176

Hanson, D. R. and Lovejoy, E. R.: Measurement of the thermodynamics of the hydrated dimer and trimer of sulfuric acid, J. Phys. Chem. A, 110, 9525–9528, doi:10.1021/jp062844w, 2006. 2176

Jacobson, M. Z.: Fundamentals of atmospheric modeling, Cambridge University Press, 1999. 2174

Kerminen, V.-M. and Kulmala, M.: Analytical formulae connecting the ”real” and the ”apparent” nucleation rate and the nuclei number concentration for atmospheric nucleation events, J. Aer. Sci., 33, 609–622, doi:10.1016/S0021-8502(01)00194-X, 2002. 2185

Lauer, A., Hendricks, J., Ackermann, I., Schell, B., Hass, H., and Metzger, S.: Simulating aerosol microphysics with the ECHAM/MADE GCM - Part I: Model description and comparison with observations, Atmospheric Chemistry & Physics, 5, 3251–3276, 2005. 2184

Lovejoy, E. R., Curtius, J., and Froyd, K. D.: Atmospheric ion-induced nucleation of sulfuric acid and water, J. Geophys. Res., 109, D08204, doi:10.1029/2003JD004460, 2004. 2174, 2177

Ma, X. and von Salzen, K.: Dynamics of the sulphate aerosol size distribution on a global scale, J. Geophys. Res., 111, D08 206, doi:10.1029/2005JD006620, 2006. 2184

Modgil, M. S., Kumar, S., Tripathi, S. N., and Lovejoy, E. R.: A parameterization of ion-induced nucleation of sulphuric acid and water for atmospheric conditions, J. Geophys. Res., 110, D19205, doi:10.1029/2004JD005475, 2005. 2171, 2184

Vehkamäki, H., Kulmala, M., Napari, I., Lehtinen, K. E. J., Timmreck, C., Noppel, M., and Laaksonen, A.: An improved parameterization for sulfuric acid-water nucleation rates for tropospheric and stratospheric conditions, J. Geophys. Res., 107, 4622, doi:10.1029/2002JD002184, 2002. 2170, 2184

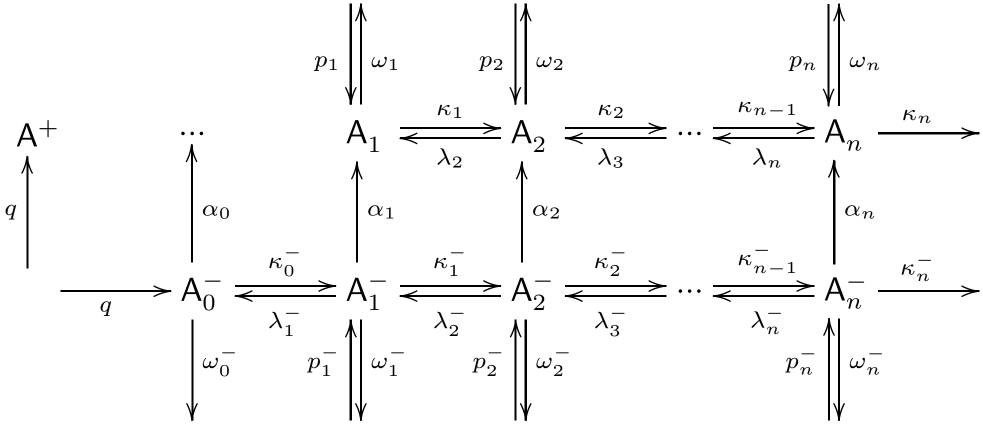

Fig. 1. Reaction scheme of a coupled neutral and charged aerosol system.

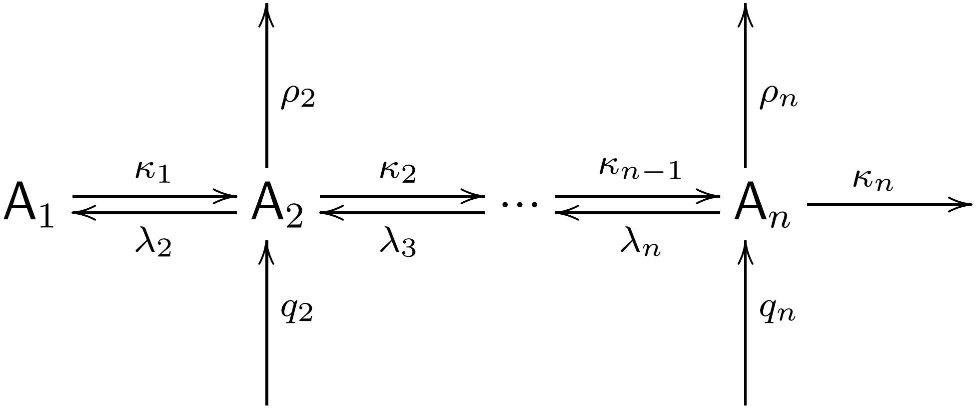

Fig. 2. Reaction scheme of a neutral aerosol system.

Title Page
Abstract
Introduction
Conclusions
References
Tables
Figures
◀❙
▶❙
◀
▶
Back
Close
Full Screen / Esc

Printer-friendly Version

Interactive Discussion

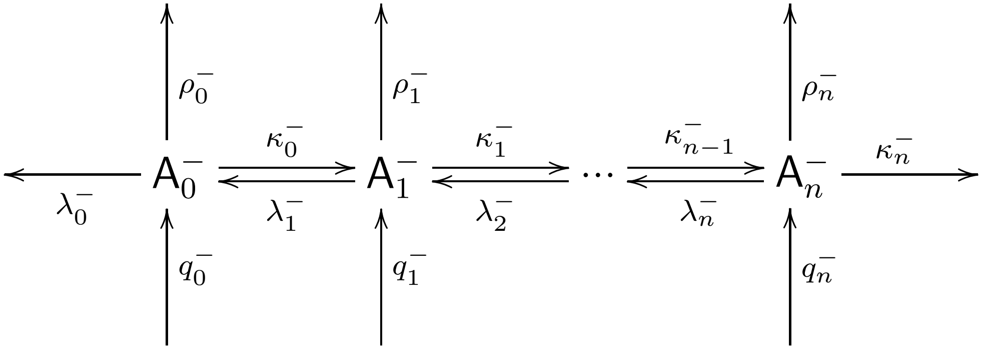

Fig. 3. Reaction scheme of a charged aerosol system.

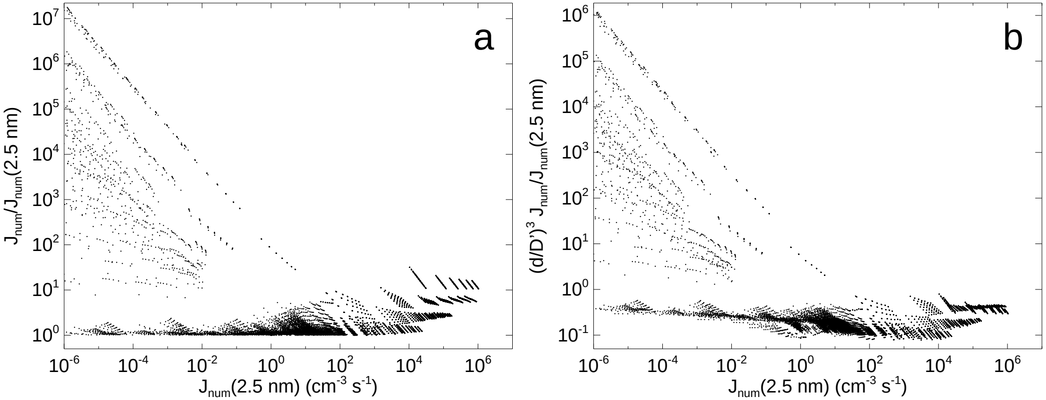

Fig. 4. **(a)** Comparison of the nucleation rate J_{num} with the formation rate $J_{\mathrm{num}}(2.5\ \mathrm{nm})$ of particles exceeding 2.5 nm in diameter. **(b)** Comparison of the nucleation rate J_{num}, scaled with the factor $(d/D')^3$, with the formation rate $J_{\mathrm{num}}(2.5\ \mathrm{nm})$ of particles exceeding 2.5 nm in diameter. d is the diameter of the smallest supercritical particle in given conditions, D' the diameter of the smallest particle exceeding 2.5 nm. All formation rates were calculated with a numerical aerosol model. The same approach for computing the rate coefficients is used in all cases.

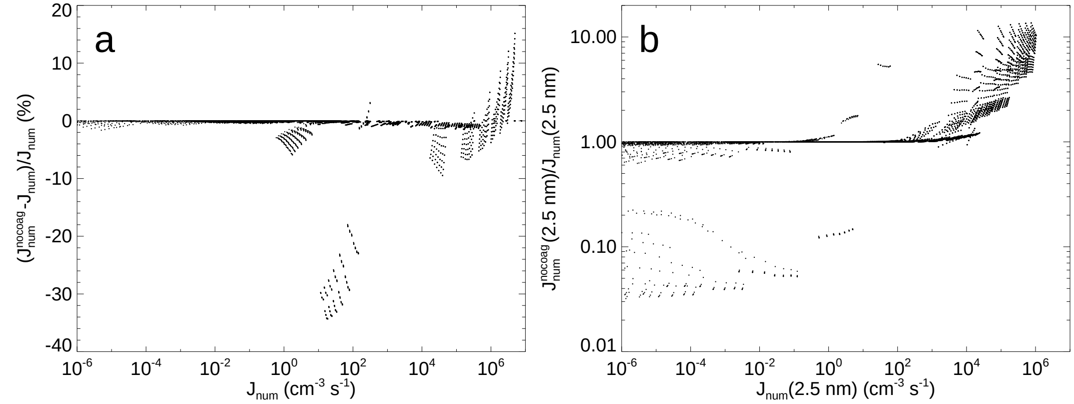

Fig. 5. **(a)** Comparison of the nucleation rate J_{num}^{nocoag}, calculated without coagulation of the nucleating particles, with the nucleation rate J_{num}, calculated with coagulation acting both as a sink for the particles as well as a contribution to the nucleation rate. **(b)** Comparison of the formation rate $J_{num}^{nocoag}(2.5\ nm)$ of particles exceeding 2.5 nm in diameter, calculated without coagulation of the forming particles, with the formation rate $J_{num}(2.5\ nm)$ of particles exceeding 2.5 nm in diameter, calculated with coagulation acting both as a sink for the particles as well as a contribution to the particle formation rate. All formation rates were calculated with a numerical aerosol model. The same approach for computing the rate coefficients is used in all cases.

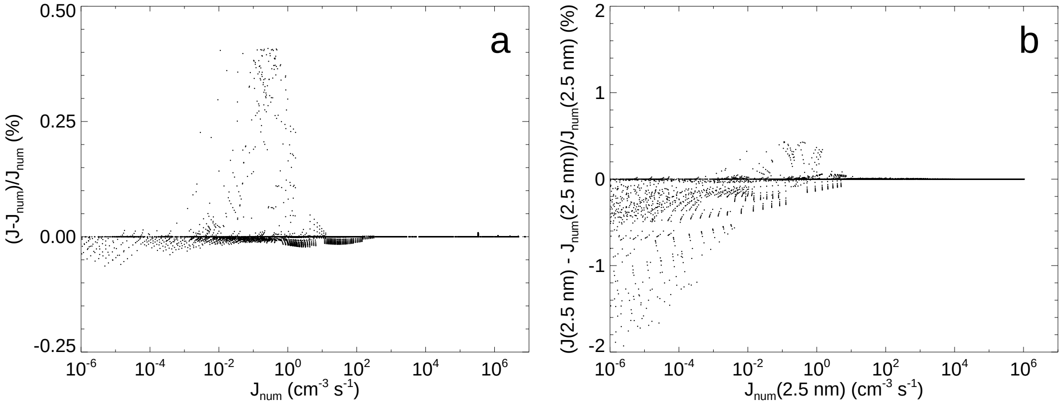

Fig. 6. **(a)** Comparison of the nucleation rate J, calculated with our semi-analytical method, with the nucleation rate J_{num} calculated with a numerical aerosol model. **(b)** Comparison of the formation rate $J(2.5\,nm)$ of aerosol particles exceeding 2.5 nm in diameter, calculated with our semi-analytical method, with the nucleation rate $J_{num}(2.5\ nm)$ calculated with a numerical aerosol model. The same approach for computing the rate coefficients is used in all cases.

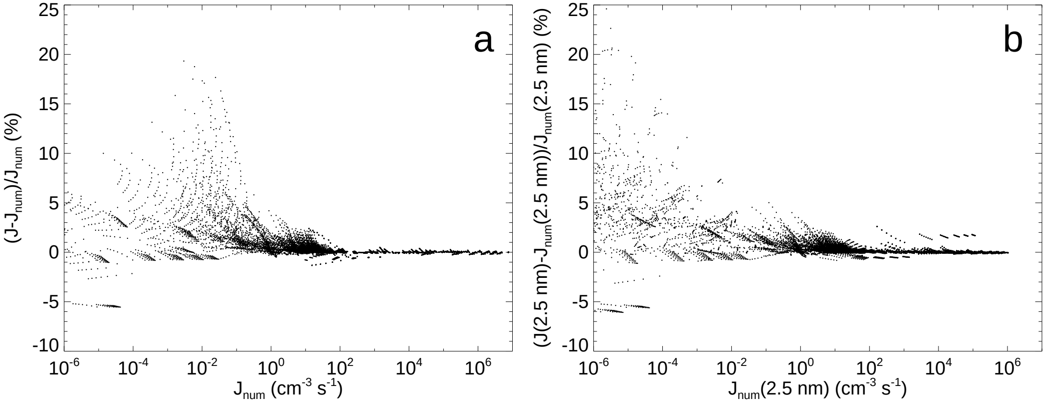

Fig. 7. **(a)** Comparison of the nucleation rate J, calculated with our semi-analytical method, with the nucleation rate J_{num}, calculated with a numerical aerosol model. **(b)** Comparison of the formation rate $J(2.5\,\text{nm})$ of aerosol particles exceeding 2.5 nm in diameter, calculated with our semi-analytical method, with the nucleation rate $J_{num}(2.5\,\text{nm})$, calculated with a numerical aerosol model. The semi-analytical method uses parameterized H_2SO_4 uptake and loss rate coefficients and average particle H_2O contents, while the numerical model calculates the rate coefficients and average particle H_2O contents from scratch.